applied sciences

MDPI

Article

Estimation of the Induction Motor Stator and Rotor Resistance Using Active and Reactive Power Based Model Reference Adaptive System Estimator

Szymon Antoni Bednarz and Mateusz Dybkowski *

Department of Electrical Machines, Drives and Measurements, Wrocław University of Science and Technology, Smoluchowskiego 19, 50-370 Wrocław, Poland; szymon.bednarz@pwr.edu.pl

* Correspondence: mateusz.dybkowski@pwr.edu.pl

Received: 30 October 2019; Accepted: 25 November 2019; Published: 27 November 2019

Featured Application: The presented parameters estimation method of an induction motor can be implemented in the applications of electric vehicles, traction systems and safety-critical drive systems. The method is based on signals which are easy to measure in the scalar and vector controlled drives.

Abstract: In this paper an induction motor parameters estimator, based on the Model Reference Adaptive System (MRAS), is presented and described. A comprehensive literature study on MRAS type parameters estimators for induction motors is also provided. The authors propose a novel PQ-MRAS estimator concept which enables the simultaneous calculation of stator and rotor resistances in the induction machine, which is its major advantage over previous investigations. The estimator employs the active (P) and reactive (Q) power of the machine which is calculated by the only measurable signals, such as stator voltage and current. The paper includes a detailed description of the proposed estimator. The PQ-MRAS was tested for various operating conditions of a drive system with the induction motor. The results obtained from computer simulation tests were verified on the laboratory set up with a DS1202 card.

Keywords: induction motor; parameter estimation; stator resistance; rotor resistance; model reference adaptive system; active power; reactive power

1. Introduction

The estimation of induction motor (IM) parameters is an essential research topic in the investigations on electrical drive systems, especially in the case of drives requiring high operational performance and precision. Modern control methods, such as the Direct Field Oriented Control (DFOC) and the Direct Torque Control (DTC) require the information about the internal state variables of the motor. Such signals as an electromagnetic flux, torque (or rotational speed for fully sensorless drives) cannot be measured directly, therefore they are estimated [1–3]. A major fraction of state variable estimators requires accurate knowledge about machine parameters [1,4]. The most crucial parameters of the induction motor is stator winding resistance and rotor winding resistance which fluctuate due to temperature variations of the machine [5,6]. Other important parameters encompass inductances, but they are immune to temperature variations [5].

The information about motor parameters values can be used also for the condition monitoring of machines [7,8]. One of the used diagnostic methods is the assumption that the fluctuations of parameters can indicate a machine fault [9] (rotor bars rupture for squirrel-cage motors or stator windings short-circuit).

Recently, numerous methods for induction motor parameters estimation have been developed. In general, they can be subdivided into two main categories [5]:

- Off-line estimators—parameters are calculated at the standstill state of the machine (self-commissioning drives), these methods are often called parameters identification methods;
- On-line estimators—parameters are calculated during the normal operation of the machine. These methods are based mostly on: Kalman Filters [10], state observers [11], MRAS [5,12] or spectral techniques [5].

The paper discusses MRAS based estimators, therefore in the further part of the introduction a brief description of this estimation method is given. A typical MRAS estimator (Figure 1) includes two basic subsystems which calculate the same base signal in different ways [12] (the same base signal is expressed by two mathematical models):

- Reference model which should be independent of the estimated parameter;
- Adjustable model which is directly (sometimes indirectly) influenced by the estimated parameter.

The general idea of this estimation algorithm relies on the minimization of the error between a reference and adjustable model by an adaptation mechanism. If the estimated parameter is equal to its reference value, the error becomes minimized.

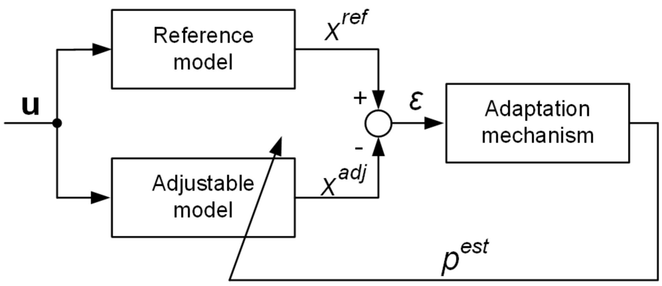

Figure 1. General idea of MRAS type parameter estimator (**u**—input signals vector, x^{ref}—reference value of chosen signal, x^{adj}—adjustable (estimated) value of chosen signal, p^{est}—estimated parameter, ε—error between reference and adjustable model).

From the base signal standpoint, MRAS type parameter estimators can be classified into several major categories:

- Electromagnetic flux-based (F-MRAS)—proposed for the first time in [13] for speed estimation. An estimator of this type can be used in stator resistance [14] or rotor resistance estimation [15], due to the fact that it consists of two basic estimators of the flux: a voltage model and a current model. The former depends directly on the stator resistance value, therefore it is used as an adjustable model in F-MRAS stator resistance estimators (in that case the current model is the reference). The current model depends directly on the rotor resistance, hence it is used as an adjustable model in F-MRAS rotor resistance estimators (then the voltage model is the reference). The major shortcomings of F-MRAS estimators are that neither of the models is a measurable quantity; estimators directly depend on both resistances simultaneously, however, only one of them can be estimated.
- Reactive power-based (Q-MRAS)—proposed in [16] for rotor resistance estimation. This estimator is independent of stator resistance. It is implemented mainly in a synchronous reference frame (x-y), which requires the estimation of synchronous speed. The reference and adjustable models use internal signals from the control structure as inputs. Quite frequently, a simplified adjustable model is used (based on control method assumptions). This results in the strong dependence of estimator operation on the control system performance. In [17], an estimator was implemented in stationary reference frame (α-β), therefore it was based only on measurable signals—independently of the internal signals from a control scheme. In [18] Q-MRAS was proposed for speed estimation.

- Active power based (P-MRAS)—proposed in [19] for stator resistance estimation. Similarly to Q-MRAS, it is implemented only in the synchronous reference frame (x-y), which determines a strong reliance on the control structure performance. In [20] a semi-active power estimator is proposed to improve robustness on rotor resistance variation. In [21] it was used for rotor resistance estimation.
- X based (X-MRAS)—proposed in [22] for stator resistance estimation. Here X is a fictitious quantity based on stator voltage and current. It was implemented only in a synchronous reference frame. It can be used for synchronous speed estimation [22].
- PY based (PY-MRAS)—proposed in [23] for stator resistance estimation. It relies on the active power and Y which is a fictitious quantity (based on stator voltage and current). The major benefit of this estimator is that the adjustable model is independent of the rotor speed. However, only simulation results were presented.
- Electromagnetic torque (T-MRAS)—proposed in [21] for rotor resistance estimation. Its major shortcoming is the fact that both reference and adjustable models are non-measurable quantities. The reference model depends on the stator resistance.
- Back electromagnetic force (back-EMF MRAS)—proposed in [18] for speed estimation. In [24] it was proposed for the stator resistance estimation. Its major advantage is that pure integration is not required through the implementation of the estimator. The reference model depends directly on rotor resistance. In [25], an improvement of estimator stability was proposed. However, the estimator employs an internal signal from the control structure (implemented in the (x-y) reference frame).

To sum up, MRAS based estimators for induction motor parameters have been developed in the last few decades. As a result, it is possible to estimate the stator or rotor resistance of a machine. However, the research on a MRAS type estimator which enables the estimation of both resistances simultaneously is still insufficient. In [26], an F-MRAS type estimator was proposed for the simultaneous estimation of rotor and stator resistance, and also the estimation of motor rotational speed. The major drawback of the proposed approach is the fact that both (adjustable and reference) models are directly dependent on the estimated parameters. Therefore, incorrect estimation of at least one parameter may deteriorate the performance of the entire estimator. Additionally, both models of the proposed MRAS are not measurable signals, in consequence it is not possible to check how calculated signals correspond to their real values—estimated parameters are calculated using estimated signals.

This article presents a new PQ-MRAS estimator which enables the estimation of both resistances simultaneously. It is based on the active and reactive powers of the induction motor. The main benefits of proposed estimator are that reference models are calculated using only measurable signals, such as current, voltage and rotor speed. In the paper, the estimator was tested for different conditions through computer simulations as well as experimental tests.

It is necessary to point out that the approaches based on the Kalman Filter enable a simultaneous, highly accurate estimation of motor parameters and state variables [27,28]. However, this method is characterized by high computational requirements and a complicated design process. These are its major drawbacks compared to MRAS systems.

A MRAS estimator is a system which is easy to parametrize and can be quickly implemented on simple microprocessor systems. The main goal of the research was to develop an estimation system that is easier to tune than the commonly known estimators. It was assumed that only simple state variable simulators would be used to develop such a system. Complex observers or EKFs cannot be compared with such systems. All systems have their pros and cons.

The article is composed of several sections. In Section 2 a mathematical model of an induction motor as well as a detailed description of the PQ-MRAS estimator are presented [29]. Section 3 includes the explanation of the vector control structure for the induction motor, while Section 4 the results of simulation tests and experimental verification. Section 5 discusses the obtained results.

2. Mathematical Models of the Induction Motor and the PQ-MRAS Estimator

In this section the mathematical models of an induction motor and a PQ-MRAS estimator are presented. A detailed description of the proposed estimator is also provided.

2.1. Mathematical Model of the Induction Motor

The model of the three-phase squirrel cage induction motor can be expressed in the stationary reference frame (α-β) by the following equations [1]:

$$\frac{\mathrm{d}\boldsymbol{\psi}_{\mathbf{s}}}{\mathrm{dt}} = \mathbf{u_s} - R_s\mathbf{i_s}, \tag{1}$$

$$\frac{\mathrm{d}\boldsymbol{\psi}_{\mathbf{r}}}{\mathrm{dt}} = -R_r\mathbf{i_r} + \mathrm{j}p_b\omega_m\boldsymbol{\psi}_{\mathbf{r}}, \tag{2}$$

$$\mathbf{i}_s = \frac{L_r}{w}\boldsymbol{\psi}_{\mathbf{s}} - \frac{L_m}{w}\boldsymbol{\psi}_{\mathbf{r}}, \tag{3}$$

$$\mathbf{i_r} = \frac{L_s}{w}\boldsymbol{\psi}_{\mathbf{r}} - \frac{L_m}{w}\boldsymbol{\psi}_{\mathbf{s}}. \tag{4}$$

$$t_e = \frac{3}{2}p_b\mathrm{Im}\{\boldsymbol{\psi}_{\mathbf{s}}^* \cdot \mathbf{i_s}\} \tag{5}$$

$$\frac{\mathrm{d}\omega_m}{\mathrm{dt}} = \frac{1}{J}(t_e - t_l) \tag{6}$$

where $\mathbf{u_s} = u_{s\alpha} + \mathrm{j}u_{s\beta}$—stator voltage vector, $\mathbf{i_s} = i_{s\alpha} + \mathrm{j}i_{s\beta}$—stator current vector, $\mathbf{i_r} = i_{r\alpha} + \mathrm{j}i_{r\beta}$—rotor current vector, $\boldsymbol{\psi}_{\mathbf{r}} = \psi_{r\alpha} + \mathrm{j}\psi_{r\beta}$—rotor electromagnetic flux vector, $\boldsymbol{\psi}_{\mathbf{s}} = \psi_{s\alpha} + \mathrm{j}\psi_{s\beta}$—stator electromagnetic flux vector, ω_m—rotational shaft speed, t_e—electromagnetic torque, t_l—load torque. R_s, R_r—stator, rotor resistances respectively; L_s, L_r, L_m—stator, rotor, magnetizing inductances, respectively; p_b—number of pole pairs, J—inertia of the shaft, $w = L_sL_r - L_m{}^2$.

It is necessary to point out that in the presented model, such phenomena as motor losses and magnetic saturation are not considered.

2.2. Mathematical Model of the PQ-MRAS Estimator

The proposed estimator consists of two subsystems:

- P-MRAS—based on the active power (P) of the machine; it is used to calculate the stator resistance.
- Q-MRAS—based on the reactive power (Q) of the machine; it is used to calculate the rotor resistance.

Each subsystem has its own independent adaptation mechanism based on a PI (proportional–integral) controller. The common part of P and Q-MRAS is the rotor flux estimator.

A reference model of the P-MRAS is given by:

$$P^{\mathrm{ref}} = \mathrm{Re}\left\{\mathbf{u_s} \cdot \mathbf{i_s}^*\right\} = u_{s\alpha}i_{s\alpha} + u_{s\beta}i_{s\beta} \tag{7}$$

In an adjustable model, estimated stator voltage is used instead of the measured one. Based on Equations (1), (3) and (4), the estimated stator voltage vector can be expressed as:

$$\mathbf{u_s}^{\mathrm{est}} = R_s\mathbf{i_s} + \frac{L_m}{L_r}\frac{\mathrm{d}\boldsymbol{\psi}_{\mathbf{r}}{}^{\mathrm{est}}}{\mathrm{dt}} + \sigma L_s\frac{\mathrm{d}\mathbf{i_s}}{\mathrm{dt}} \tag{8}$$

Finally, the formula of P-MRAS adjustable model is:

$$P^{\mathrm{adj}} = \mathrm{Re}\left\{\mathbf{u_s}^{\mathrm{est}} \cdot \mathbf{i_s}^*\right\} = R_s{}^{\mathrm{est}}\left(i_{s\alpha}{}^2 + i_{s\beta}{}^2\right) + \sigma L_s\left(i_{s\alpha}\frac{\mathrm{d}i_{s\alpha}}{\mathrm{dt}} + i_{s\beta}\frac{\mathrm{d}i_{s\beta}}{\mathrm{dt}}\right) + \frac{L_m}{L_r}\left(i_{s\alpha}\frac{\mathrm{d}\psi_{ra}{}^{\mathrm{est}}}{\mathrm{dt}} + i_{s\beta}\frac{\mathrm{d}\psi_{r\beta}{}^{\mathrm{est}}}{\mathrm{dt}}\right) \tag{9}$$

It can be observed that the value of active power, calculated by the adjustable model, directly depends on stator resistance. Therefore, the role of stator resistance adaptation mechanism is the minimization of the error between the two models:

$$\varepsilon_{\mathrm{P}} = P^{\mathrm{ref}} - P^{\mathrm{adj}}, \tag{10}$$

$$R_{\mathrm{s}}{}^{\mathrm{est}} = K_{PRs}\varepsilon_P + K_{IRs}\int \varepsilon_P \mathrm{d}t \tag{11}$$

where K_{PRs}, K_{IRs}—coefficients of the proportional and integral terms, respectively.

Rotor flux components in (9) are derived from the current model estimator [1]:

$$\psi_{\mathbf{r}}{}^{\mathrm{est}} = \int \left(\frac{R_r}{L_r}\left(L_m\mathbf{i}_{\mathbf{s}} - \psi_{\mathbf{r}}{}^{\mathrm{est}}\right) + jp_b\omega_m\psi_{\mathbf{r}}{}^{\mathrm{est}}\right)\mathrm{d}t. \tag{12}$$

The reference model of the Q-MRAS is given by:

$$Q^{\mathrm{ref}} = \mathrm{Im}\{\mathbf{u}_{\mathrm{s}} \cdot \mathbf{i}_{\mathrm{s}}{}^*\} = u_{s\beta}i_{s\alpha} - u_{s\alpha}i_{s\beta}, \tag{13}$$

whereas the adjustable model of this subsystem uses the estimated value of the stator voltage (8):

$$Q^{\mathrm{adj}} = \mathrm{Im}\left\{\mathbf{u}_{\mathrm{s}}{}^{\mathrm{est}} \cdot \mathbf{i}_{\mathrm{s}}{}^*\right\} = \sigma L_{\mathrm{s}}\left(i_{s\alpha}\frac{\mathrm{d}i_{s\beta}}{\mathrm{d}t} - i_{s\beta}\frac{\mathrm{d}i_{s\alpha}}{\mathrm{d}t}\right) + \frac{L_m}{L_r}\left(i_{s\alpha}\frac{\mathrm{d}\psi_{r\beta}^{\mathrm{est}}}{\mathrm{d}t} - i_{s\beta}\frac{\mathrm{d}\psi_{r\alpha}^{\mathrm{est}}}{\mathrm{d}t}\right). \tag{14}$$

In this model the dependence on the rotor resistance is implicit. It consists of the rotor flux components which are calculated by the current model (12) which directly depends on the value of this parameter. The rotor resistance adaptation mechanism minimizes the error between the reference and adjustable models:

$$\varepsilon_Q = \left|Q^{ref}\right| - \left|Q^{adj}\right|, \tag{15}$$

$$R_r{}^{\mathrm{est}} = K_{PRr}\varepsilon_Q + K_{IRr}\int \varepsilon_Q \mathrm{d}t. \tag{16}$$

where K_{PRr}, K_{IRr}—coefficients of the proportional and integral terms, respectively. The sign of the reactive power is changed due to the shaft rotational speed reversals, therefore in the adaptation mechanism the absolute values of Q^{ref} and Q^{adj} are used. In Figure 2 a block diagram of the PQ-MRAS estimator is shown.

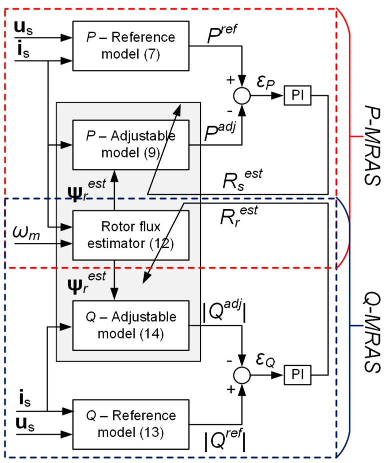

Figure 2. Scheme of the PQ-MRAS estimator.

3. Description of the Vector Control Structure for Induction Motor

During the tests, the induction motor was controlled by a closed-loop vector control structure known as the Direct Field Oriented Control—DFOC. A block diagram of the control structure is shown in Figure 3.

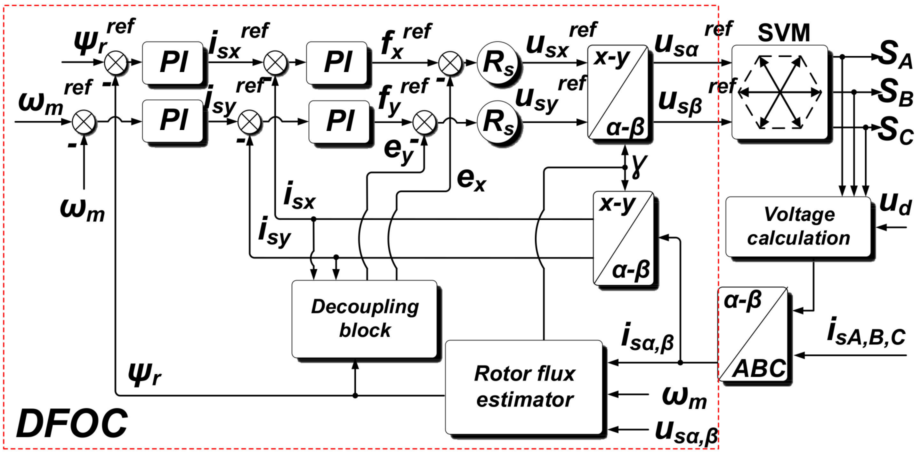

Figure 3. Scheme of the DFOC system.

This method involves the independent control of the flux and torque of the machine by two decoupled control paths [6]. The implementation of this control method requires the transformation of the stator current vector to the synchronous reference frame (x-y) rotating with the speed of the rotor flux vector. The rotor flux is controlled by the i_{sx} component of the stator current, whereas the electromagnetic torque is controlled by the i_{sy} stator current component. The reference frame transformation requires the information about the actual position of the rotor flux vector. During the simulation and experimental tests, the current model was used for the rotor flux vector estimation [1]:

$$\psi_{\mathbf{r}}^{\mathbf{i}} = \int \left(\frac{R_r}{L_r} \left(L_m \mathbf{i_s} - \psi_{\mathbf{r}}^{\mathbf{i}} \right) + jp_b \omega_m \psi_{\mathbf{r}}^{\mathbf{i}} \right) \mathrm{d}t. \tag{17}$$

Instead of the current model, the voltage model can be used in the vector controlled IM drives for rotor or stator flux estimation:

$$\psi_{\mathbf{r}}^{v} = \frac{L_r}{L_m} \int (\mathbf{u_s} - R_s \mathbf{i_s}) \mathrm{d}t - \frac{w}{L_m} \mathbf{i_s}, \tag{18}$$

This estimator directly depends on the stator resistance value. Therefore, it can be used to evaluate P-MRAS operation in the closed-loop mode.

Voltage vector components were calculated using control signals and measured DC bus voltage from a Voltage Source Inverter (VSI):

$$u_{s\alpha} = \frac{2}{3} u_{\mathrm{d}} \left(S_A - \frac{1}{2} (S_B + S_C) \right), \tag{19}$$

$$u_{s\beta} = \frac{\sqrt{3}}{3} u_d (S_B + S_C). \tag{20}$$

The PQ-MRAS estimator can operate in two modes (Figure 4):

- Open-loop mode—independently of the control structure;
- Closed-loop mode—coupled with the control structure; the estimated parameters are injected to the control structure (flux estimator).

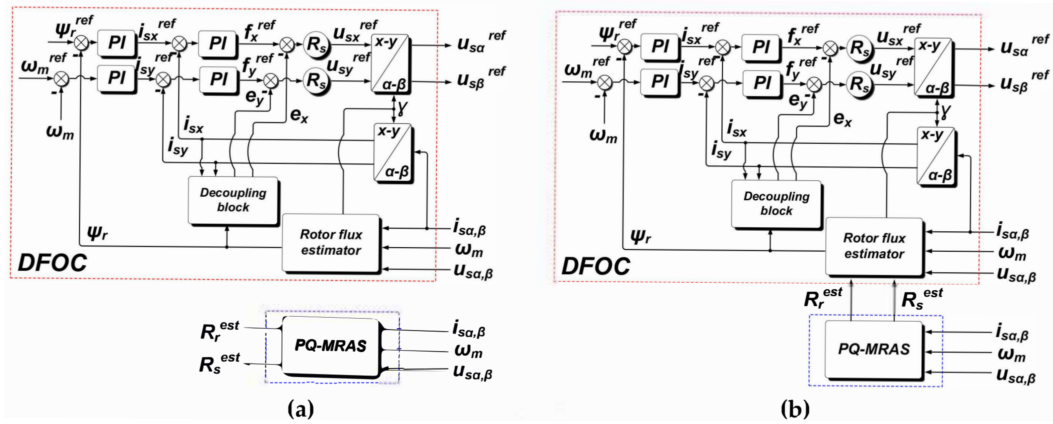

Figure 4. Operation of the PQ-MRAS estimator: (**a**) open-loop mode, (**b**) closed-loop mode.

4. Simulation and Experimental Results

This section includes the results of both the simulation tests and experimental verification of the PQ-MRAS estimator. The estimator was examined for different conditions of the drive operations, such as: load torque and speed variations (including speed reversals). The rated data of the tested induction motor are summarized in Table A1 (Appendix A). During the simulation and experimental tests, the values of adaptation mechanism coefficients were the same (Appendix B). State variables from the drive, such as: rotational speed, electromagnetic torque, rotor flux and stator current are presented along with internal signals from the PQ-MRAS estimator: active and reactive powers, estimated stator and rotor resistances. Each of the signals and state variables is normalized to its nominal value.

4.1. Simulation Results

Simulation tests were performed using MATLAB/Simulink software (version 2018b, The MathWorks, Natick, MA, USA). During the simulations, the estimator was tested for the open-loop as well as closed-loop operation modes. In a simulation model, effects such as signal offsets, measurements noise and inverter nonlinearity were not taken into consideration.

4.1.1. Operation of the PQ-MRAS in Open-Loop Mode

The main goal of the first test was to check the general performance of the PQ-MRAS. The results are presented in Figures 5 and 6. It can be observed that both estimated parameters tracked real values with high accuracy.

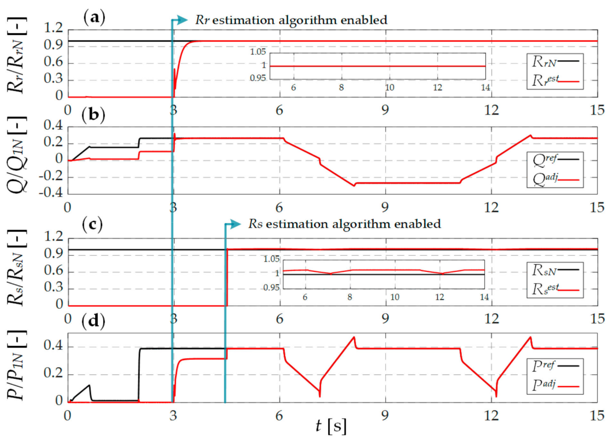

Figure 5. Operation of the PQ-MRAS estimator: (**a**) estimated rotor resistance, (**b**) reference and estimated reactive power, (**c**) estimated stator resistance, (**d**) reference and estimated active power; (simulation results), ($\omega_m{}^{ref}$ = ±0.5 ωmN, t_L = ±0.75 tN, R_r = R_{rN}, R_s = R_{sN}).

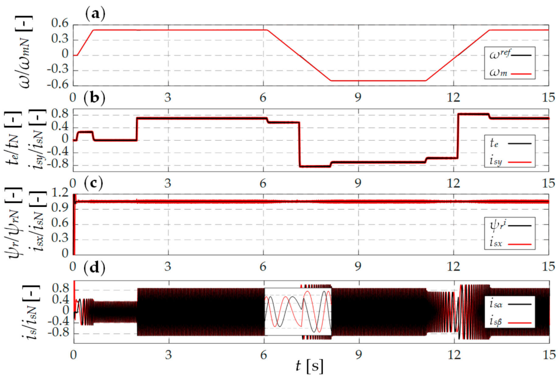

Figure 6. State variables of the drive: (**a**) reference and simulated rotational speed, (**b**) electromagnetic torque and stator current component i_{sy}, (**c**) estimated rotor flux vector module and stator current component i_{sx}, (**d**) stator current components $i_{s\alpha,\beta}$; (simulation results), ($\omega_m{}^{ref} = \pm 0.5\ \omega mN$, $t_L = \pm 0.75\ tN$, $R_r = R_{rN}$, $R_s = R_{sN}$).

Even during speed reversal variations the estimated parameters were negligible (maximum estimation error for stator resistance increased to 2%). During the second test, the robustness of the estimator to load torque variations was considered. The obtained results (Figures 7 and 8) show that both parameters were calculated with high accuracy even for load variations.

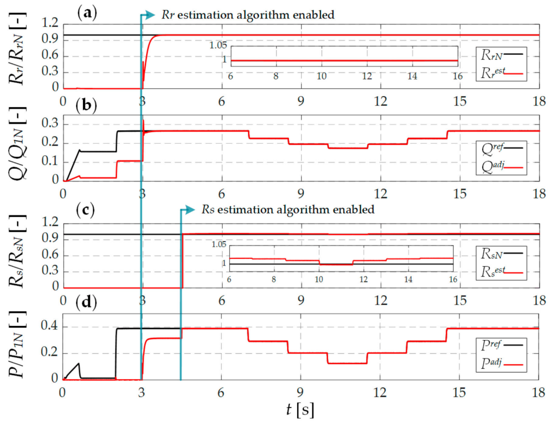

Figure 7. Operation of the PQ-MRAS estimator: (**a**) estimated rotor resistance, (**b**) reference and estimated reactive power, (**c**) estimated stator resistance, (**d**) reference and estimated active power; (simulation results), ($\omega_m{}^{ref} = 0.5\ \omega mN$, t_L = var, $R_r = R_{rN}$, $R_s = R_{sN}$).

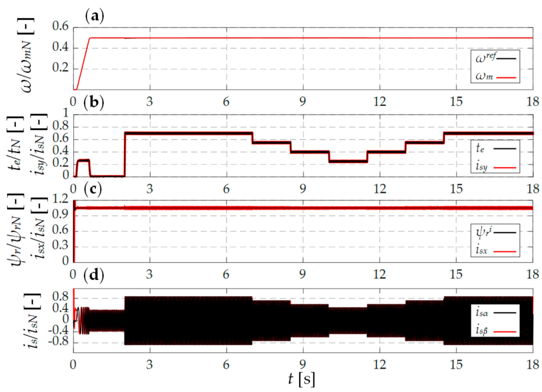

Figure 8. State variables of the drive: (**a**) reference and simulated rotational speed, (**b**) electromagnetic torque and stator current component i_{sy}, (**c**) estimated rotor flux vector module and stator current component i_{sx}, (**d**) stator current components $i_{s\alpha,\beta}$; (simulation results), ($\omega_m{}^{ref} = 0.5\ \omega mN$, t_L = var, $R_r = R_{rN}$, $R_s = R_{sN}$).

The aim of the next analysis was to check how the values of adaptation mechanism coefficients impact the estimator performance. Figure 9 shows a comparison of estimator signals for different sets of coefficients: nominal values (Appendix B), nominal values multiplied by 5 and nominal values divided by 5. The coefficient values have a major impact on the dynamics of the estimator, nevertheless it operated in a stable manner.

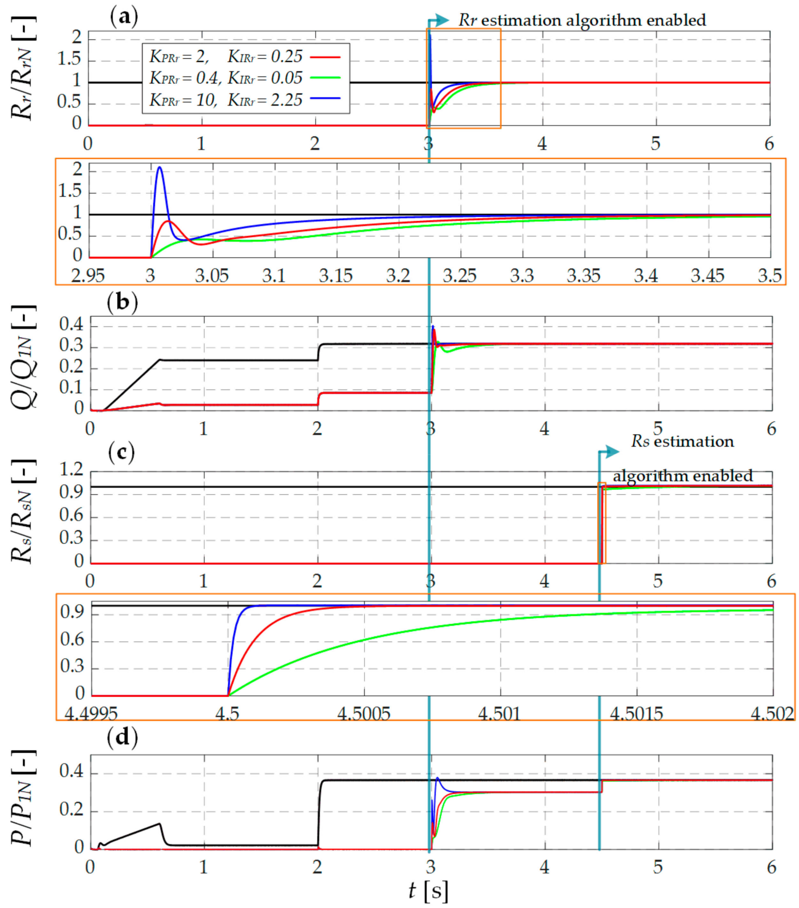

Figure 9. Operation of the PQ-MRAS estimator for different values of parameters in adaptation mechanisms: (**a**) estimated rotor resistance, (**b**) reference and estimated reactive power, (**c**) estimated stator resistance, (**d**) reference and estimated active power; (simulation results), ($\omega_m{}^{ref}$ = 0.5 ωmN, t_L = 0.75 tN, $R_r = R_{rN}$, $R_s = R_{sN}$).

During the next test, it was assumed that both resistances increased up to 150% of their nominal values, which was related to the changes of machine windings temperatures. It can be seen that both resistances were estimated correctly (Figure 10). Due to rotor resistance variations, the estimation error of the rotor flux can be observed (Figure 11), because the current model is directly influenced by this parameter (17). The inaccurate calculation of the rotor flux vector results in the coupling of flux and torque control paths, which consequently results in the deterioration of drive performance.

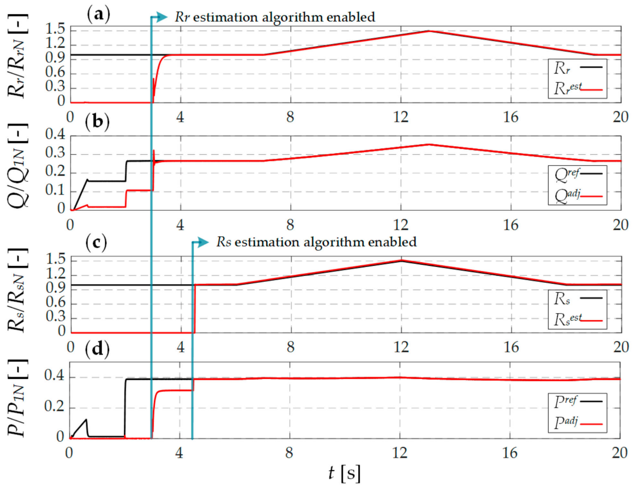

Figure 10. Operation of the PQ-MRAS estimator: (**a**) estimated rotor resistance, (**b**) reference and estimated reactive power, (**c**) estimated stator resistance, (**d**) reference and estimated active power; (simulation results), ($\omega_m{}^{ref}$ = 0.5 ωmN, t_L = 0.75 tN, R_r = var, R_s = var).

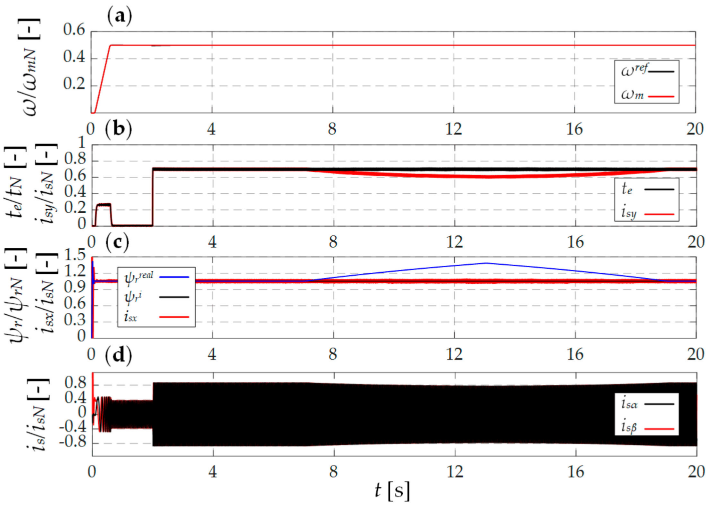

Figure 11. State variables of the drive: (**a**) reference and measured rotational speed, (**b**) electromagnetic torque and stator current component i_{sy}, (**c**) estimated rotor flux vector module and stator current component i_{sx}, (**d**) stator current components $i_{s\alpha,\beta}$; (simulation results), ($\omega_m{}^{ref}$ = 0.5 ωmN, t_L = 0.75 tN, R_r = var, R_s = var).

4.1.2. Operation of the PQ-MRAS in Closed-Loop Mode

During further tests, the estimator was operating in the closed-loop mode. Both estimated parameters tracked their real values (Figure 12).The estimated value of the rotor resistance was injected into the control system (to the rotor flux estimator—to the current model) at t = 12 s. It resulted in the elimination of the flux error estimation and the decoupling of the control paths (Figure 13).

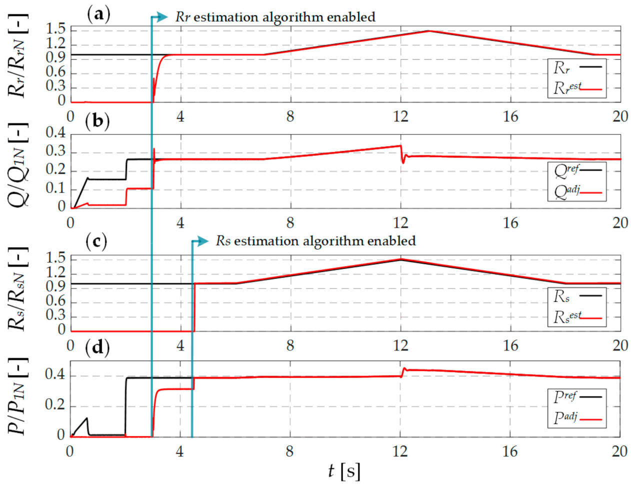

Figure 12. Operation of the PQ-MRAS estimator: (**a**) estimated rotor resistance, (**b**) reference and estimated reactive power, (**c**) estimated stator resistance, (**d**) reference and estimated active power; (simulation results), (ω_m^{ref} = 0.5 ωmN, t_L = 0.75 tN, R_r = var, R_s = var).

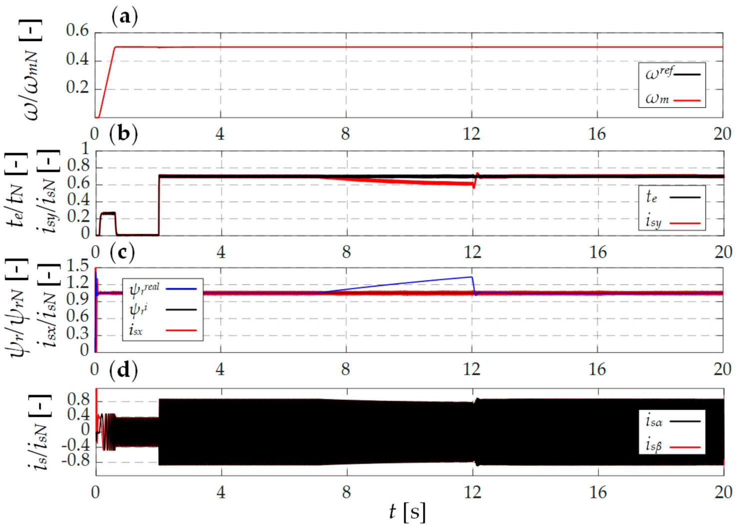

Figure 13. State variables of the drive: (**a**) reference and measured rotational speed, (**b**) electromagnetic torque and stator current component i_{sy}, (**c**) estimated rotor flux vector module and stator current component i_{sx}, (**d**) stator current components $i_{s\alpha,\beta}$; (simulation results), (ω_m^{ref} = 0.5 ωmN, t_L = 0.75 tN, R_r = var, R_s = var).

A similar study was performed with a voltage model [1] instead of the current model as the estimator of the rotor flux (18). This estimator directly depends on the stator resistance value (current model depends on rotor resistance). Therefore, it can be used to evaluate P-MRAS operation in the closed-loop mode. The estimated stator resistance was injected into the control system at t = 11 s, which resulted in the improvement of the rotor flux estimation accuracy (Figures 14 and 15).

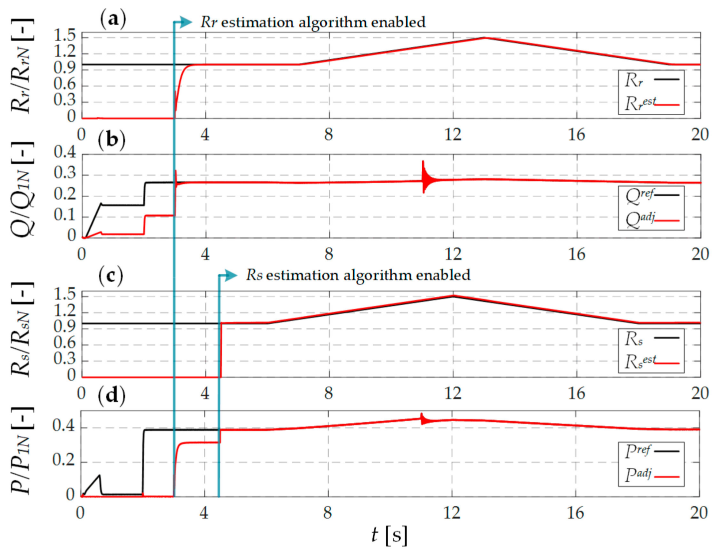

Figure 14. Operation of the PQ-MRAS estimator: (**a**) estimated rotor resistance, (**b**) reference and estimated reactive power, (**c**) estimated stator resistance, (**d**) reference and estimated active power; (simulation results), ($\omega_m{}^{ref}$ = 0.5 ωmN, t_L = 0.75 tN, R_r = var, R_s = var).

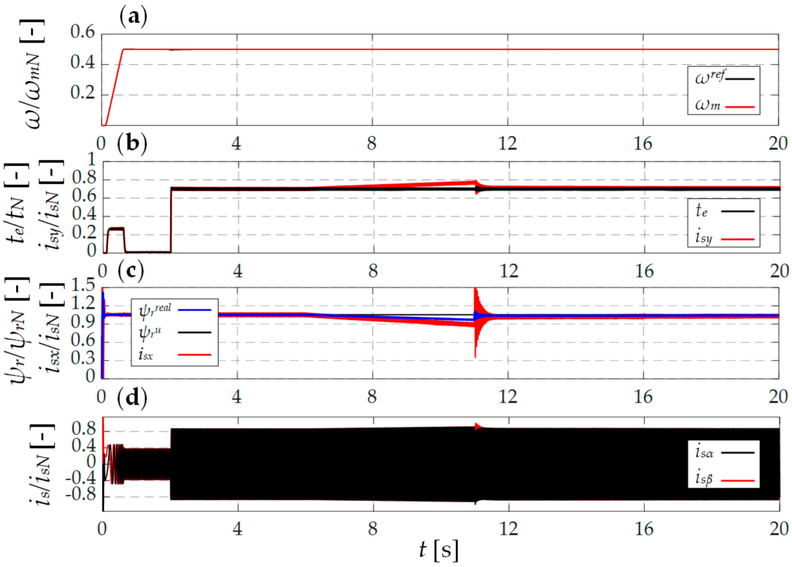

Figure 15. State variables of the drive: (**a**) reference and measured rotational speed, (**b**) electromagnetic torque and stator current component i_{sy}, (**c**) estimated rotor flux vector module and stator current component i_{sx}, (**d**) stator current components $i_{s\alpha,\beta}$; (simulation results), ($\omega_m{}^{ref}$ = 0.5 ωmN, t_L = 0.75 tN, R_r = var, R_s = var).

4.2. Experimental Results

The experimental verification of the PQ-MRAS estimator was carried out on the laboratory setup shown in Figure 16. The setup consisted of two induction motors coupled by a clutch—one motor was controlled by the DFOC algorithm, the other one worked as a load. The control algorithm and PQ-MRAS were implemented in a rapid prototyping unit dSPACE MicroLabBox (dSPACE Inc., Wixom, MI, USA) through the MATLAB/Simulink software (version 2015b, The MathWorks). The drive system was controlled in real-time by an application created in the ControlDesk software (version 5.4, dSPACE Inc., Wixom, MI, USA).

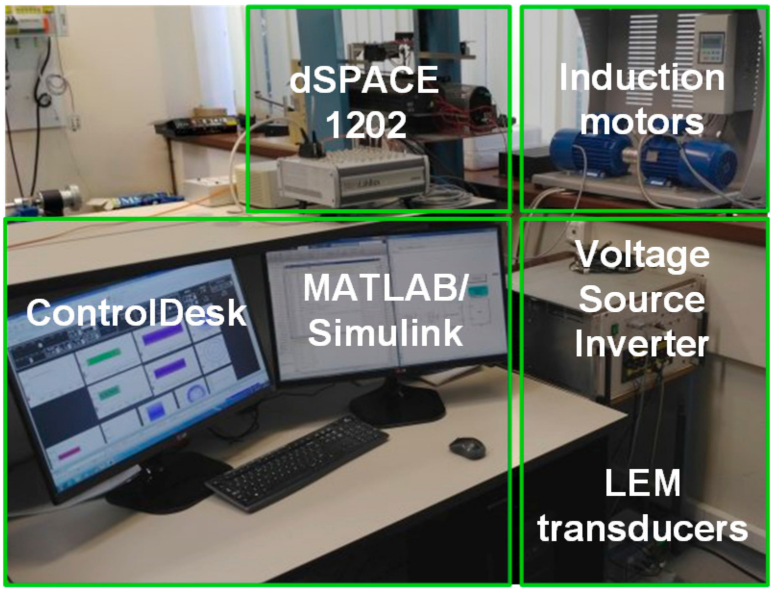

Figure 16. Photography of the experimental setup.

During the experiments, the estimator was tested for the open-loop operation mode. The rotor flux vector was estimated by the current model, whereas an electromagnetic torque was calculated by:

$$t_e{}^{est} = \frac{3}{2} p_b \frac{L_m}{L_r} \mathrm{Im}\left\{ \psi_{\mathbf{r}}^{\mathbf{i}*} \cdot \mathbf{i_s} \right\}. \tag{21}$$

During the first test, the general performance of the PQ-MRAS was analyzed. It can be observed that the obtained results correspond with the simulation results (Figures 17 and 18). It should be noted, however, that neither of the estimated parameters exactly matched its nominal values. Nevertheless, the estimation error for rotor resistance was about 5% and for stator resistance it was about 10%.

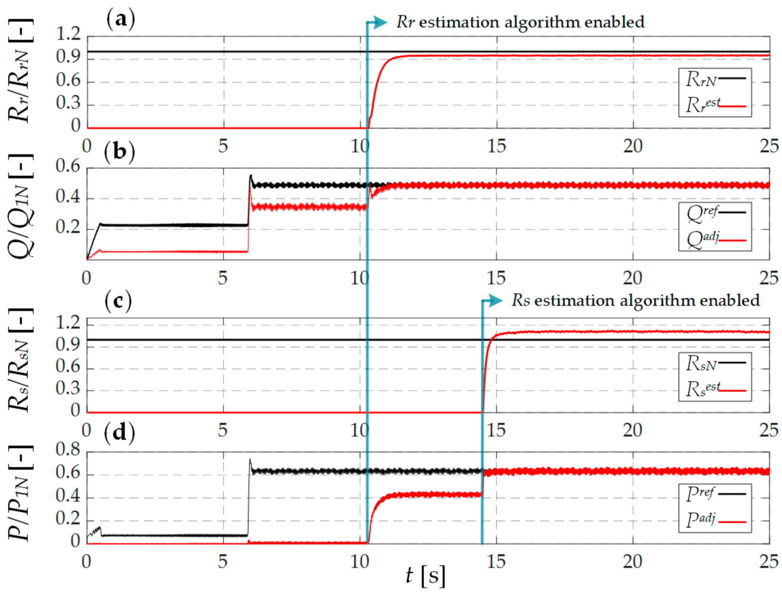

Figure 17. Operation of the PQ-MRAS estimator: (**a**) estimated rotor resistance, (**b**) reference and estimated reactive power, (**c**) estimated stator resistance, (**d**) reference and estimated active power; (experimental results), ($\omega_m{}^{ref}$ = 0.5 ωmN, t_L = 0.75 tN).

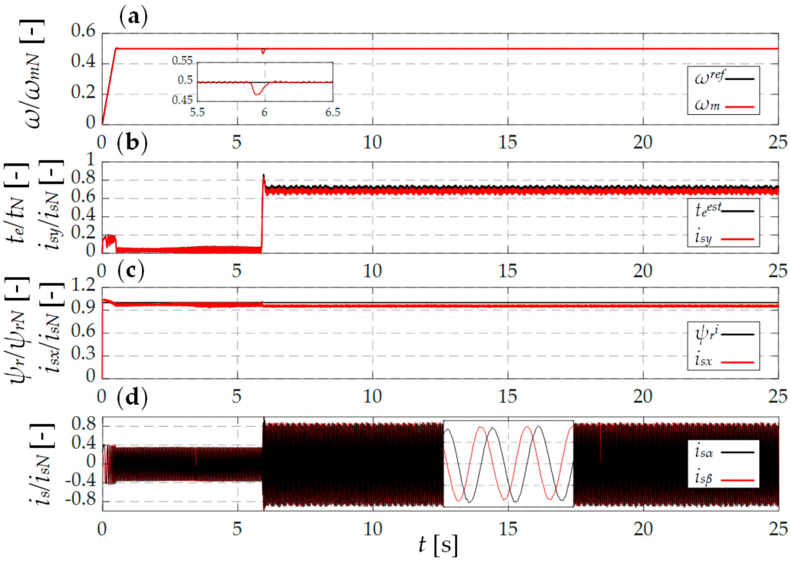

Figure 18. State variables of the drive: (**a**) reference and measured rotational speed, (**b**) electromagnetic torque and stator current component i_{sy}, (**c**) estimated rotor flux vector module and stator current component i_{sx}, (**d**) stator current components $i_{s\alpha,\beta}$; (experimental results), ($\omega_m{}^{ref} = 0.5\,\omega mN$, $t_L = 0.75\ tN$).

The main aim of the second test was to check estimator robustness to load torque variations (Figures 19 and 20). The values of both estimated resistances fluctuated according to load variations but in limited ranges (3% for rotor resistance, 5% for stator resistance).

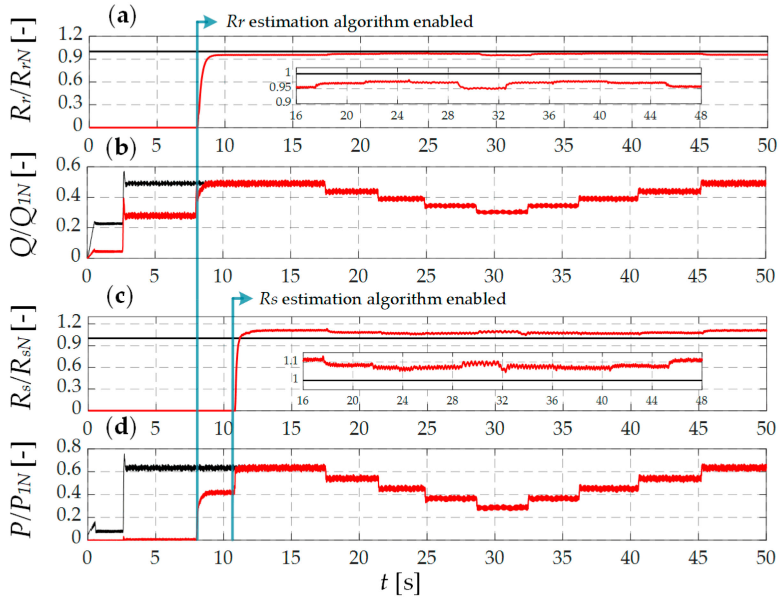

Figure 19. Operation of the PQ-MRAS estimator: (**a**) estimated rotor resistance, (**b**) reference and estimated reactive power, (**c**) estimated stator resistance, (**d**) reference and estimated active power; (experimental results), ($\omega_m{}^{ref} = 0.5\ \omega mN$, t_L = var).

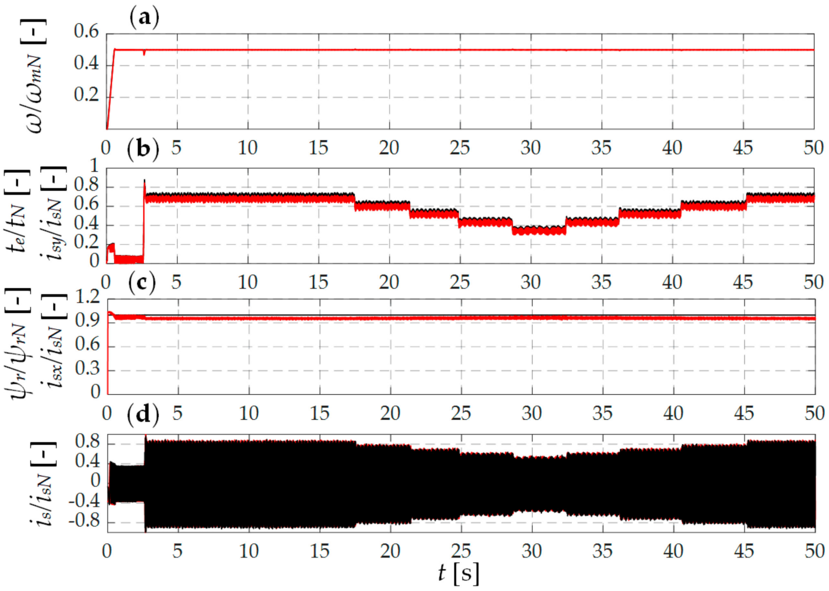

Figure 20. State variables of the drive: (**a**) reference and measured rotational speed, (**b**) electromagnetic torque and stator current component i_{sy}, (**c**) estimated rotor flux vector module and stator current component i_{sx}, (**d**) stator current components $i_{s\alpha,\beta}$; (experimental results), ($\omega_m{}^{ref} = 0.5\ \omega mN$, t_L = var).

Subsequently, a speed reversal test was carried out (Figures 21 and 22). The estimator operated stably, yet the fluctuations of estimated parameters were noticeable—especially during transients (about 5% for rotor resistance, ±10% for stator resistance).

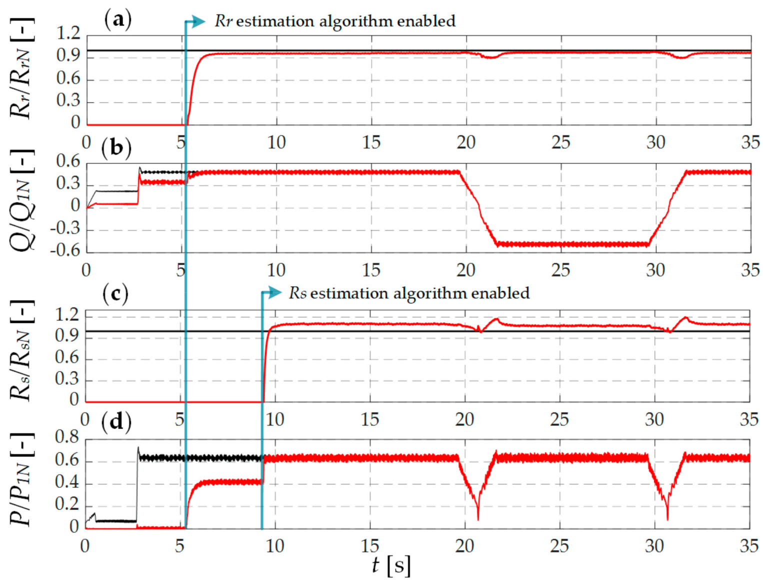

Figure 21. Operation of the PQ-MRAS estimator: (**a**) estimated rotor resistance, (**b**) reference and estimated reactive power, (**c**) estimated stator resistance, (**d**) reference and estimated active power; (experimental results), ($\omega_m{}^{ref} = \pm 0.5\ \omega mN$, $t_L = \pm 0.75\ tN$).

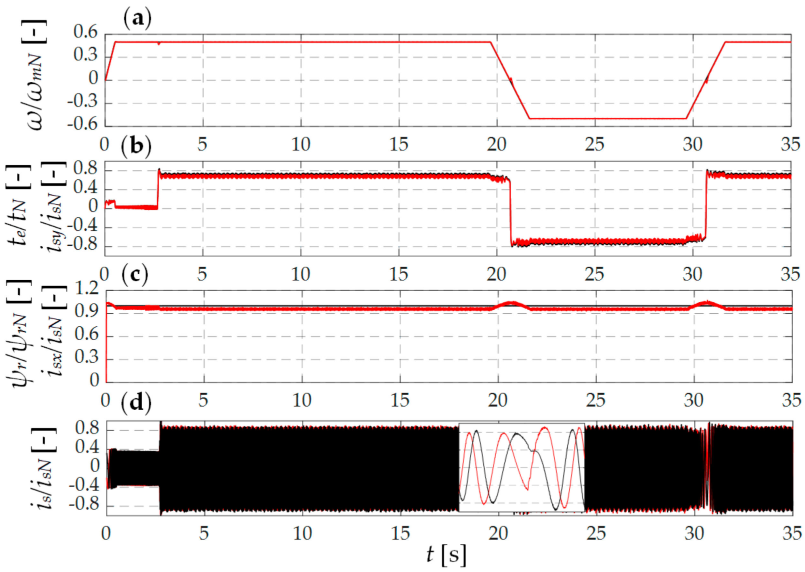

Figure 22. State variables of the drive: (**a**) reference and measured rotational speed, (**b**) electromagnetic torque and stator current component i_{sy}, (**c**) estimated rotor flux vector module and stator current component i_{sx}, (**d**) stator current components $i_{s\alpha,\beta}$; (experimental results), ($\omega_m{}^{ref}$ = ±0.5 ωmN, t_L = ±0.75 tN).

During the last test, the influence of the values of adaptation mechanisms coefficients on the estimator operation was analyzed. The coefficients were changed it the same way as during the simulation test. A noticeable influence on the dynamics was visible, however, the estimator operated stably for each of the sets of parameters (Figure 23).

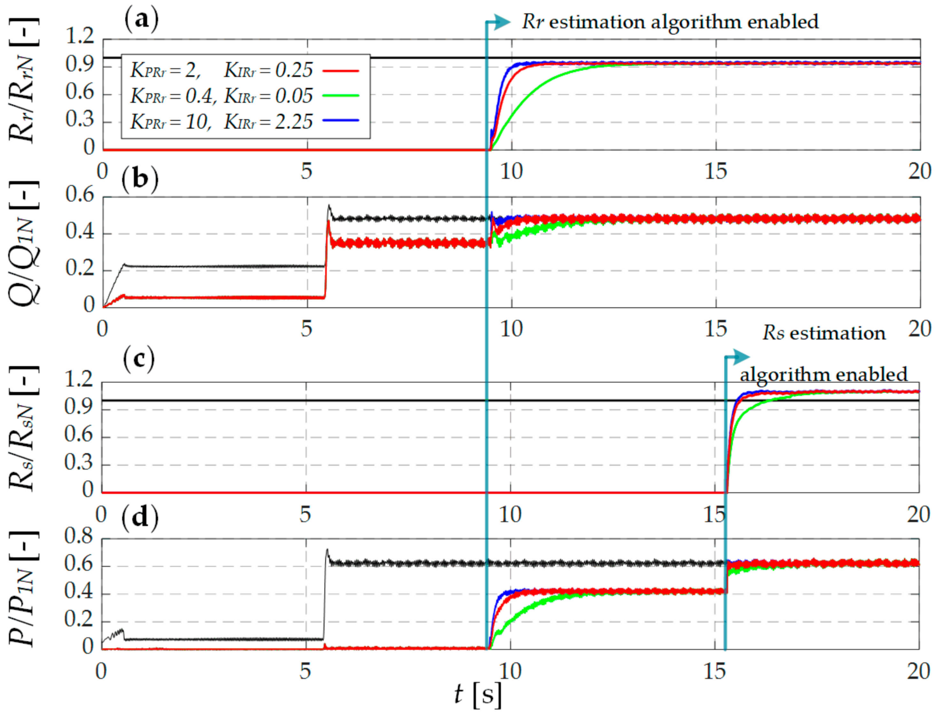

Figure 23. Operation of the PQ-MRAS estimator for different values of parameters in adaptation mechanisms: (**a**) estimated rotor resistance, (**b**) reference and estimated reactive power, (**c**) estimated stator resistance, (**d**) reference and estimated active power; (experimental results), ($\omega_m{}^{ref}$ = 0.5 ωmN, t_L = 0.75 tN).

5. Discussion

Based on the presented results, it can be concluded that the experimental results correspond with those obtained through simulations. It should be noted that the estimation errors of resistances were greater for experiments than for simulations, however, they did not exceed 10%. These discrepancies resulted from the simplifications of the simulation model.

Nevertheless, the main contributions of the presented research as regards MRAS estimators are:

- simultaneous estimation of stator and rotor resistance;
- estimator requires only measurable input signals (independence of the control structure).

Additional attributes of the presented estimator include:

- stable estimation during speed reversals (including zero-speed range) and load torque variations;
- estimation of parameters during steady-states and transients;
- variations of adaptation mechanism coefficients impact only subsystem dynamics; the estimator works stably.

Further research directions will focus on employing an analytical method to adaptation mechanism coefficients setting. The impact of other parameters, such as inductances, on the estimator performance will be also taken into the consideration.

Author Contributions: Conceptualization, S.A.B., M.D.; methodology, S.A.B., M.D.; software, S.A.B.; validation, M.D., S.A.B.; formal analysis, M.D.; investigation, S.A.B., M.D.; resources, S.A.B., M.D.; data curation, S.A.B.; writing—original draft preparation, S.A.B.; writing—review and editing, M.D.; visualization, S.A.B.; supervision, M.D.; project administration, M.D.; funding acquisition, M.D.

Funding: This research was funded by statutory funds of the Faculty of Electrical Engineering of the Wroclaw University of Science and Technology under grant number 049M/0004/19.

Conflicts of Interest: The authors declare no conflict of interest.

Abbreviations and Symbols

MRAS	Model Reference Adaptive System
IM	Induction Motor
DFOC	Direct Field Oriented Control
DTC	Direct Torque Control
VSI	Voltage Source Inverter
P	Active Power
Q	Reactive Power
$\mathbf{u_s}$	Stator Voltage Vector
$\mathbf{i_s}$	Stator Current Vector
$\mathbf{i_r}$	Rotor Current Vector
$\boldsymbol{\psi_s}$	Stator Electromagnetic Flux Vector
$\boldsymbol{\psi_r}$	Rotor Electromagnetic Flux Vector
ω_m	Rotational Shaft Speed
t_e	Electromagnetic Torque
t_l	Load Torque
R_s	Stator Resistance
R_r	Rotor Resistance
L_s	Stator Inductance
L_r	Rotor Inductance
L_m	Magnetizing Inductance
p_b	Number of Pole Pairs
J	Shaft Inertia
ε_P	Estimation Error of the Active Power
ε_Q	Estimation Error of the Reactive Power
K_{PRs}	Coefficient of the Proportional Term in the Stator Resistance Adaptation Mechanism
KI_{Rs}	Coefficient of the Integral Term in the Stator Resistance Adaptation Mechanism
K_{PRr}	Coefficient of the Proportional Term in the Rotor Resistance Adaptation Mechanism
KI_{Rr}	Coefficient of the Integral Term in the Rotor Resistance Adaptation Mechanism

Appendix A

Table A1. IM Data.

Symbol	Rated Data	Value	Unit
P_N	Power	1.1	kW
U_N	Stator voltage	400	V
I_N	Stator current	2.8	A
n_N	Mechanical speed	1360	rpm
tN	Torque	7.7	Nm
R_s	Stator resistance	5.9	Ω
R_r	Rotor resistance	4.5	Ω
L_s	Stator inductance	451.0	mH
L_r	Rotor inductance	451.0	mH
L_m	Magnetizing inductance	424.4	mH
J	Inertia	0.0143	kg·m^2
p_b	Pole pairs	2	-
η	Efficiency	0.79	-

Appendix B

Table A2. Coefficients of PI controllers in adaptation mechanism.

Symbol	Value
K_{PRs}	10
KI_{Rs}	20
K_{PRr}	2
KI_{Rr}	0.25

References

1. Holtz, J. Sensorless Control of Induction Motor Drives. *Proc. IEEE* **2002**, *90*, 1359–1394. [CrossRef]
2. Pascas, M. Sensorless Drives in Industrial Applications. *IEEE Ind. Electron. Mag.* **2011**, *5*, 16–23. [CrossRef]
3. Bao, D.; Wang, H.; Wang, X.; Zhang, C. Sensorless Speed Control Based on the Improved Q-MRAS Method for Induction Motor Drives. *Energies* **2018**, *11*, 235. [CrossRef]
4. Chen, B.; Yao, W.; Chen, F.; Lu, Z. Parameter Sensitivity in Sensorless Induction Motor Drives with the Adaptive Full-Order Observer. *IEEE Trans. Ind. Electron.* **2015**, *62*, 4307–4318. [CrossRef]
5. Toliyat, H.A.; Levi, E.; Raina, M. A review of RFO induction motor parameter estimation techniques. *IEEE Trans. Energy Convers.* **2003**, *18*, 271–283. [CrossRef]
6. Kazmierkowski, M.P.; Krishann, F.; Blabjerg, F. *Control in Power Electronics: Selected Problems*, 1st ed.; Academic Press: San Diego, CA, USA, 2002.
7. Iserman, R. *Fault-Diagnosis Applications: Model-Based Condition Monitoring: Actuators, Drives, Machinery, Plants, Sensors, and Fault-Tolerant Systems*, 1st ed.; Springer: Berlin/Heidelberg, Germany, 2011.
8. Merizalde, Y.; Hernández-Callejo, L.; Duque-Perez, O. State of the art and trends in the monitoring, detection and diagnosis of failures in electric induction motors. *Energies* **2017**, *10*, 1056. [CrossRef]
9. Bednarz, S.A.; Dybkowski, M. Induction Motor Windings Faults Detection Using Flux-error Based MRAS Estimators. *Diagnostyka* **2019**, *20*, 87–92. [CrossRef]
10. Barut, M.; Demir, R.; Zerdali, E.; Inan, R. Real-time implementation Speed-sensorless, of bi input-extended Kalman filter-based estimator for control of induction motors. *IEEE Trans. Ind. Electron.* **2012**, *59*, 4197–4206. [CrossRef]
11. Kubota, H.; Matsuse, K.; Nakano, T. DSP-Based Speed Adaptive Flux Observer of Induction Motor. *IEEE Trans. Ind. Appl.* **1993**, *29*, 344–348. [CrossRef]
12. Syam, P.; Kumar, R.; Das, S.; Chattopadhyay, A.K. Review on model reference adaptive system for sensorless vector control of induction motor drives. *IET Electr. Power Appl.* **2015**, *9*, 496–511. [CrossRef]

13. Schauder, C. Adaptive Speed Identification for Vector Control of Induction Motors Without Rotational Transducers. *IEEE Trans. Ind. Appl.* **1992**, *28*, 1054–1061. [CrossRef]
14. Vasic, V.; Vukosavic, S.N.; Levi, E. A stator resistance estimation scheme for speed sensorless rotor flux oriented induction motor drives. *IEEE Trans. Energy Convers.* **2003**, *18*, 476–483. [CrossRef]
15. Zorgani, Y.A.; Koubaa, Y.; Boussak, M. Sensorless speed control with MRAS for induction motor drive. In Proceedings of the 20th International Conference on Electrical Machines (ICEM), Marseille, France, 2–5 September 2012. [CrossRef]
16. Garces, L.J. Parameter Adaption for the Speed-Controlled Static AC Drive with a Squirrel-Cage Induction Motor. *IEEE Trans. Ind. Appl.* **1980**, *IA-16*, 173–178. [CrossRef]
17. Naït Saïd, M.S.; Benbouzid, M.E.H. Induction motors direct field oriented control with robust on-line tuning of rotor resistance. *IEEE Trans. Energy Convers.* **1999**, *14*, 1038–1042. [CrossRef]
18. Peng, F.; Fukao, T. Robust speed identification for speed-sensorless vector control of induction motors. *IEEE Trans. Ind. Appl.* **1994**, *30*, 1234–1240. [CrossRef]
19. Perng, S.; Lai, Y.; Liu, C. Sensorless vector controller for induction motor drives with parameter identification. In Proceedings of the 24th Annual Conference of the IEEE Industrial Electronics Society (IECON), Aachen, Germany, 31 August–4 September 1998. [CrossRef]
20. Madadi Kojabadi, H.; Abarzadeh, M.; Aghaei Farouji, S. Robust stator resistance identification of an IM drive using model reference adaptive system. *Energy Convers. Manag.* **2013**, *65*, 507–517. [CrossRef]
21. Mapelli, F.L.; Tarsitano, D.; Cheli, F. A rotor resistance MRAS estimator for EV induction motor traction drive based on torque and reactive stator power: Simulation and experimental results. In Proceedings of the 2014 International Conference on Electrical Machines (ICEM), Berlin, Germany, 2–5 September 2014. [CrossRef]
22. Ravi Teja, A.V.; Chakraborty, C.; Maiti, S.; Hori, Y. A new model reference adaptive controller for four quadrant vector controlled induction motor drives. *IEEE Trans. Ind. Electron.* **2012**, *59*, 3757–3767. [CrossRef]
23. Basak, S.; Ravi Teja, A.V.; Chakraborty, C.; Hori, Y. A new model reference adaptive formulation to estimate stator resistance in field oriented induction motor drive. In Proceedings of the 39th Annual Conference of the IEEE Industrial Electronics Society (IECON), Vienna, Austria, 10–13 November 2013. [CrossRef]
24. Zhen, L.; Xu, L. Sensorless field orientation control of induction machines based on a mutual MRAS scheme. *IEEE Trans. Ind. Electron.* **1998**, *45*, 824–831. [CrossRef]
25. Rashed, M.; Stronach, A.F. A stable back-EMF MRAS-based sensorless low-speed induction motor drive insensitive to stator resistance variation. *IEE Proc. Electr. Power Appl.* **2004**, *151*, 685–693. [CrossRef]
26. Zerikat, M.; Chekroun, S.; Mechernene, A. A robust MRAS-sensorless scheme based rotor and stator resistance estimation of a direct vector controlled induction motor drive. In Proceedings of the 2011 16th International Conference on Methods and Models in Automation and Robotics, Miedzyzdroje, Poland, 22–25 August 2011. [CrossRef]
27. Talla, J.; Peroutka, Z.; Blahnik, V.; Strejt, L. Rotor and stator resistance estimation of induction motor mased on augmented EKF. In Proceedings of the 2015 International Conference on Applied Electronics, Pilsen, Czech Republic, 8–9 September 2015.
28. Demir, R.; Barut, M.; Yildiz, R.; Inan, R.; Zerdali, E. EKF based rotor and stator resistance estimations for direct torque control of Induction Motors. In Proceedings of the 2017 International Conference on Optimization of Electrical and Electronic Equipment (OPTIM) and International Aegean Conference on Electrical Machines and Power Electronics (ACEMP), Brasov, Romania, 25–27 May 2017.
29. Dybkowski, M.; Bednarz, S.A. Simultaneous Estimation of the Stator and Rotor Resistances in an Induction Motor Drive using Novel Active and Reactive Power Based Model Reference Adaptive System. In Proceedings of the 2019 International Conference on Electrical Drives and Power Electronics (EDPE), The High Tatras, Slovakia, 24–26 September 2019. [CrossRef]